Talanta 83 (2010) 379–385

Contents lists available at ScienceDirect

Talanta

journal homepage: www.elsevier.com/locate/talanta

PdNi- and Pd-coated electrodes prepared by electrodeposition from ionic liquid for nonenzymatic electrochemical determination of ethanol and glucose in alkaline media

Hsin-Yi Huang, Po-Yu Chen*

Department of Medicinal and Applied Chemistry, Kaohsiung Medical University, Kaohsiung City 807, Taiwan

ARTICLE INFO

Article history:
Received 30 July 2010
Received in revised form
22 September 2010
Accepted 23 September 2010
Available online 1 October 2010

Keywords:
Nonenzymatic electrochemical electrode
Ionic liquid
Electrodeposition
Palladium nickel
Ethanol
Glucose

ABSTRACT

Nonenzymatic electrochemical determination of ethanol and glucose was respectively achieved using PdNi- and Pd-coated electrodes prepared by electrodeposition from the novel metal-free ionic liquid (IL); *N*-butyl-*N*-methylpyrrolidinium dicyanamide (BMP-DCA). BMP-DCA provided an excellent environment and wide cathodic limit for electrodeposition of metals and alloys because many metal chlorides could dissolve in this IL where the reduction potentials of Pd(II) and Ni(II) indeed overlapped, leading to the convenience of potentiostatic codeposition. In aqueous solutions, the reduction potentials of Pd(II) and Ni(II) are considerably separated. The bimetallic PdNi coatings with atomic ratios of ~80/20 showed the highest current for ethanol oxidation reaction (EOR). Ethanol was detected by either cyclic voltammetry (CV) or hydrodynamic amperometry (HA). Using CV, the dependence of EOR peak current on concentration was linear from 4.92 to 962 μM with a detection limit of 2.26 μM ($\sigma = 3$), and a linearity was observed from 4.92 to 988 μM using HA (detection limit 0.83 μM ($\sigma = 3$)). The Pd-coated electrodes prepared by electrodeposition from BMP-DCA showed electrocatalytic activity to glucose oxidation and CV, HA, and square-wave voltammetry (SWV) were employed to determine glucose. SWV showed the best sensitivity and linearity was observed from 2.86 μM to 107 μM, and from 2.99 mM to 10.88 mM with detection limits of 0.78 μM and 25.9 μM ($\sigma = 3$), respectively. For glucose detection, the interference produced from ascorbic acid, uric acid, and acetaminophen was significantly suppressed, compared with a regular Pt disk electrode.

1. Introduction

Electrochemical sensors for ethanol [1] and glucose [2] usually took advantage of the relevant enzymes to selectively react with ethanol or glucose to produce electroactive species that were detected to determine the concentrations of the two molecules, or to trigger the redox reaction of a cofactor and the concentrations of ethanol or glucose could be determined by detecting the current produced from the redox reaction of this cofactor. The enzymes used for electrochemical sensors are usually oxidase or dehydrogenase. If oxidase is employed, H_2O_2 was usually the electroactive species concurrently produced with the enzyme reaction. On the other hand, the redox couple of NADH/NAD^+ was usually the cofactors involved in dehydrogenase reactions and the detection of NADH/NAD^+, therefore, was used to determine the concentrations of ethanol or glucose. Direct detection of H_2O_2 or NADH/NAD^+ usually suffered by the essential high overpotential that leads to sever interference produced from other electroactive species. Indirect detection could be achieved and lower detection potentials could be applied if appropriate mediators or second enzyme is joined. No matter direct or indirect; the immobilization of enzymes and/or mediators were/was the key of preparing a successful enzyme electrode. Therefore, the loss of enzyme and/or mediator loading and degradation of enzyme activity in critical temperature or solution pH were the main concern for enzyme electrodes. However, the unique selectivity demonstrated by enzyme electrodes is undoubted.

Because of the drawbacks for enzyme electrodes, it is reasonable and practical to develop nonenzymatic electrodes for the detection of ethanol and glucose; especially in critical conditions such as very acidic, very basic, high or low temperatures in which the enzymes malfunction. Generally, for amperometric sensors, metal or alloy was usually the basic element for nonenzymatic electrodes; e.g. many metallic and alloying electrodes have been employed to detect glucose [3]. Recently, nanotechnology strengthened this concept and selectivity that usually lacked for nonenzymatic electrodes could be improved. For metallic nanoparticle or nanoporous electrodes, Ni [4] and Pd [5–7] are now the most popular elements

* Corresponding author. Tel.: +886 7 3121101x2587; fax: +886 7 3125339.
E-mail address: pyc@kmu.edu.tw (P.-Y. Chen).

0039-9140/$ – see front matter © 2010 Elsevier B.V. All rights reserved.
doi:10.1016/j.talanta.2010.09.032

used in nonenzymatic electrodes. Some of them were dispersed on carbon nanotubes (CNTs) to form metal–CNT composite film. Pt or Pd alloying nanomaterials [8,9] were also employed in nonenzymatic glucose electrodes; higher activity and lower expense were their main matter. Recently, few reports about nonenzymatic glucose sensors incorporated metal or alloy nanoparticle and ionic liquids have been published [9–11]. Except the sophisticated nanomaterials, some materials that seemed to be low technological demonstrated comparable sensitivity and selectivity in glucose detection [12,13]. Compared with the nonenzymatic electrochemical detection of glucose, ethanol detection using nonenzymatic electrodes was relatively rare. PdNi-coated Si nanowires (PdNi/SiNWs) have been employed to build an amperometric ethanol sensor [14]. Metal or alloy materials were mostly used in ethanol oxidation reaction (EOR) involved in fuel cells [15–17] and these materials are actually potent to be used in nonenzymatic ethanol electrodes.

Electrodeposition is a convenient and direct method to prepare metal and alloy-coated electrodes where nanostructures could be formed. Ionic liquids (ILs), unique designer's solvents, have approved to be good electrolytes for electrodeposition of metals and alloys because most ILs are nonvolatile, nonflammable, chemically and electrochemically stable. In addition, the properties of ILs are tunable by adjusting the composition or modifying the chemical structures of cations and/or anions. ILs are liquefiable in a wide range of temperature and hydrogen evolution can be significantly suppressed when aprotic ILs were employed [18,19]. However, hydrogen evolution is not preventable in aqueous solutions, especially for the electrodeposition of active metals. Except for the above merits and characteristics, ILs might be the most complicate solvent in the perspective of the types of intermolecular forces [20]. Because of the very complex solvating properties of ILs, the reduction potentials of metallic ions in ILs do not obey the same sequence as seen in usual electrolytes. Electrodeposition of bicomponent alloys or bimetallic coatings becomes more feasible and easier in ILs because many metal ions with very different reduction potentials in aqueous solutions (e.g. Pd(II) and Ni(II)) actually showed the overlapped reduction potentials in ILs. Based on the aforementioned, it is interesting and important to know whether the electrodeposits obtained from ILs are appropriate materials for nonenzymatic detection of ethanol and glucose.

In this study, the novel air- and water-stable IL *N*-butyl-*N*-methylpyrrolidinium dicyanamide (BMP-DCA) was employed as the electrolyte for the electrodeposition of electrocatalytic PdNi and Pd. The electrodeposition of PdNi in ILs has never been reported. However, the reports about the electrodeposition of Ni in DCA-based ILs have been published [21,22] and several ILs have been used for electrodeposition of Ni and Ni alloys [18,19]. DCA-based ILs have never been used for electrodeposition of Pd and Pd alloys; however, the electrodeposition of Pd and Pd alloys in other ILs has been reported [18,19]. The DCA-based ILs show very good solubilities to metal halides, leading to the convenience for preparing electrodepositing baths. The electrodeposited PdNi and Pd coatings were characterized with environmental scanning electron microscope (ESEM) and the atomic ratios of Pd/Ni were determined with energy dispersive spectrometer (EDS). The crystalline structures of PdNi and Pd coatings were studied with powder X-ray diffractometer (XRD). The PdNi- and Pd-coated electrodes were employed to detect ethanol and glucose using three different electrochemical methods to assess the feasibility of these metal coatings in nonenzymatic detection of ethanol and glucose in alkaline media. Alkaline media were chosen because a higher sensitivity and poisoning resistance could be obtained using these electrodes. An effort is still being paid on improving the performance of these electrodes in neutral media.

2. Experimental

2.1. Materials

N-butyl-*N*-methylpyrrolidinium dicyanamide ionic liquid (BMP-DCA IL) was prepared by following the published procedures [23]. However, 1-butylchloride from Sigma–Aldrich was employed. This IL was dried under vacuum (5×10^{-6} Torr) at 120 °C for at least 1 day. The starting materials for preparing this IL, *N*-methylpyrrolidin from Fluca and sodium dicyanamide from Acros, were used as received. $PdCl_2$, $NiCl_2$, and iron wire were purchased from Alfa Aesar. NaOH was obtained from SHOWA, acetaminophen (AP) from MP Biomedicals (Germany), and uric acid (UA) from Acros. Glucose was provided by Hayashi pure chemical industries (Japan). All aqueous solutions were prepared using deionized water purified from a Millipore system.

2.2. Instrumentation

The dried BMP-DCA IL was stored in a glove box (MBRAUN, UNI LAB-B) and the content of O_2 and H_2O was controlled under 1 ppm. Electrochemical experiments were carried out either inside the glove box using a Princeton Applied Research 263A potentiostat/galvanostat (PAR 263A) or outside the glove box using a CH Instruments electrochemical analyzer (CHI 660C). A conventional three-electrode electrochemical cell was used for voltammetric study and electrodeposition. The working electrode was a Pt disk electrode (BAS, MF-2013). For electrodeposition, a piece of iron wire or a screen-printed carbon (SPC) purchased from Zensor R&D was used as working electrode. In the glove box, a piece of Pt wire immersed in ferrocene/ferrocenium (dissolved in the IL with the molar ratio of $Fc/Fc^+ = 1$) in a glass tube with a porous tip was used as a reference electrode. The potential, therefore, was reported with respect to the redox potential of the Fc/Fc^+ when experiments were performed in IL. A counter electrode in which a Pt spiral immersed in the IL separated from the bulk solution by a porosity E glass frit was used. Outside of the glove box, an Ag/AgCl reference electrode (NaCl saturated) and a Pt wire counter electrode were used in aqueous solutions.

An FEI Quanta 400F environmental scanning electron microscope (ESEM) coupled with an energy dispersive spectrometer (EDS) was employed to examine the surface morphologies and to semi-quantitatively determine the elemental compositions of the PdNi, and Pd coatings. The crystalline structures of the PdNi, and Pd electrodeposits were analyzed with a Shimadzu XD-D1 powder X-ray diffractometer (XRD).

2.3. Procedures

$PdCl_2$ and/or $NiCl_2$ were/was introduced into BMP-DCA to prepare the bath(s) for electrodeposition of PdNi or Pd. Before the electrodeposition would be carried out, the voltammetric behavior of Pd(II), Ni(II), and their mixtures was studied, respectively. Electrodeposition of PdNi was achieved by controlled-potential electrolysis on Fe wire electrodes that were cleaned in acetone, concentrated chloric acid, and then in doubly deionized water. After electrodeposition was accomplished, the PdNi-coated Fe wire electrodes (Fe/PdNi) were immediately soaked in pure and dry acetonitrile to completely remove the residual IL; screen-printing carbon (SPC) electrode, however, was used as the substrate for the electrodeposition of Pd and the Pd-coated SPC electrode (SPC/Pd) was immersed in warm water (~60 °C) to remove IL. PdNi coatings with various atomic contents of Pd were prepared by manipulating the concentrations of Pd(II) in the mixtures of Pd(II) and Ni(II) and by adjusting the electrodepositing potentials. The Fe/PdNi electrodes were used for the nonenzymatic detection of ethanol. The

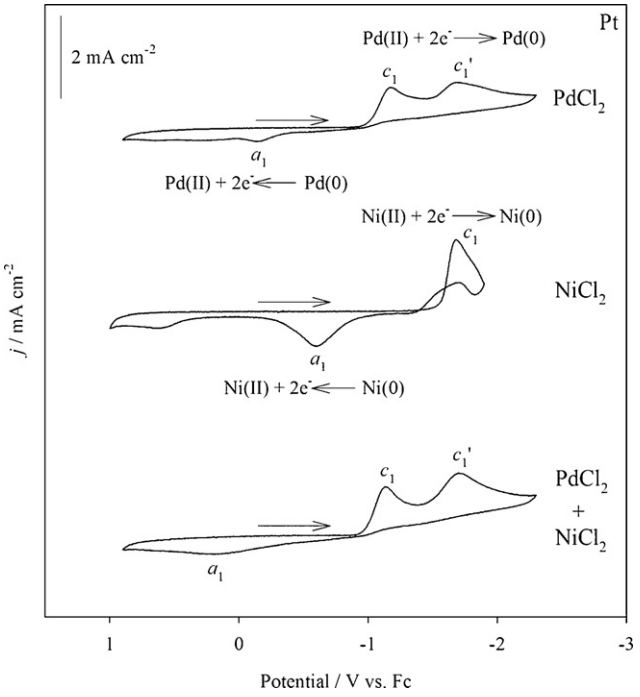

Fig. 1. Cyclic voltammograms recorded at Pt electrode in BMP-DCA ionic liquid containing 50 mM $PdCl_2$, 50 mM $NiCl_2$, or a mixture of $PdCl_2$ and $NiCl_2$ (50 mM each). Scan rate: 50 mV s^{-1}. Temperature: 313 K.

nonenzymatic detection of glucose, however, was studied using the SPC/Pd electrodes. Cyclic voltammetry (CV) and hydrodynamic amperometry (HA) were used to establish the calibration curves for ethanol and a recovery test was studied. For glucose detection, CV, HA, and square-wave voltammetry (SWV) were employed to construct the calibration curves and a recovery test was also carried out to assess the feasibility of the entire procedures.

3. Results and discussion

3.1. Voltammetric behavior of Pd(II), Ni(II), and their mixtures

Because controlled-potential electrolysis was employed to electrodeposit PdNi and Pd, the voltammetric behavior of Pd(II), Ni(II), and their mixtures must be studied in the beginning and then the appropriate electrodeposition potentials could be selected. Although the electrodeposition of PdNi and Pd was carried out at Fe electrodes (see the following sections), a Pt electrode was used for voltammetric study because Fe was galvanically replaced by Pd or Ni if it is immersed in the electroplating bath for a too long period and precise results could not be obtained. Fig. 1 shows the cyclic voltammogram of Pd(II) recorded at a Pt electrode. The potential was initially scanned in the negative direction and the Pd(II) species in BMP-DCA IL exhibited two reductive waves (c_1 and c_1'). The XRD pattern showed that the electrodeposits obtained at waves c_1 and c_1' were metallic Pd (signals at 2θ, 40.1° (1 1 1), 46.7° (2 0 0), and 68.9° (2 2 0)). Therefore, the reductive reaction of $Pd(II) + 2e^- \rightarrow Pd(0)$ was assigned to the two reductive waves. It was supposed that there were two types of Pd complex ions, leading to two reductive waves. This phenomenon has ever been reported in 1-butyl-3-methylimidazolium chloride (BMIMCl) [24]. After the potential scan was reversed, a tiny oxidative wave (a_1) was observed around 0.0 V and it was supposed that a little Pd electrodeposited on the electrode surface during the cathodic scan was reoxidized at wave a_1. However, anodic dissolution of a Pd electrode did not success in BMP-DCA; therefore, the assumption above could not be confirmed.

On the other hand, Ni(II) demonstrated a single reductive wave (c_1) assigned to the reduction reaction of $Ni(II) + 2e^- \rightarrow Ni(0)$ (Fig. 1) because the XRD pattern showed that the electrodeposits obtained at wave c_1 from the Ni(II) solution were metallic Ni (signal at 2θ, 44.4° (1 1 1)). A current loop was observed in the reversed scan, indicating that nucleation processes were involved in the reduction of Ni(II). The Ni deposits formed at reductive wave c_1 were reoxidized after the potential was reversed; the oxidative wave (a_1) was thus observed.

The aforementioned results indicated that codeposition of PdNi should be feasible because the reduction potentials of Pd(II) and Ni(II) were overlapped. This behavior is very unique because Pd(II) (from a noble metal) and Ni(II) (from an active metal) have a huge separation between their reduction potentials in aqueous solutions. BMP-DCA IL, therefore, showed its significance in controlled-potential codeposition of Pd and Ni. In Fig. 1, the cyclic voltammogram of the mixture of Pd(II) and Ni(II) showed this fact. The peak current of the reductive wave (c_1') increased with increasing the concentration of Ni(II) in the mixture of Pd(II) and Ni(II). PdNi could be easily obtained by controlled-potential electrodeposition, if the depositing potentials are applied at wave c_1'. However, PdNi with low Ni content still could be obtained when the potentials were applied at wave c_1.

3.2. Nonenzymatic electrocatalytic ethanol oxidation reaction (EOR) at Fe/Pd and Fe/PdNi electrodes

The electrodeposition of Pd and PdNi was carried out in the relevant solutions by controlled-potential electrolysis on Fe wire electrodes (Fe/Pd and Fe/PdNi electrodes). To reduce the experimental variance, the same quantity of charge (250 mC) was accumulated for the electrodeposition of Pd and PdNi on the same conductive area. Fe wire electrode was employed because this electrode was not electroactive in alkaline solutions (1.0 M NaOH) with or without ethanol (Fig. 2a); other electrodes such as Cu and W wires even showed apparent oxidative waves in the alkaline solutions without ethanol. Fig. 2b indicates that a Pd wire electrode showed a very typical behavior of electrocatalytic EOR on a metal electrode. For a comparison with the Pd wire electrode, a Fe/Pd electrode obtained by electrodeposition of Pd from BMP-DCA was used to study the voltammetric behavior in the alkaline solution with and without ethanol. As can be seen in Fig. 2c, except for the higher response that should result from the more porous surface of the Fe/Pd (see the inset of Fig. 2c), the Fe/Pd showed an almost identical voltammetric behavior as the Pd wire electrode did.

Three selected Fe/PdNi electrodes with different atomic contents of Pd were studied for their electrocatalytic behavior towards EOR and the relevant cyclic voltammograms are shown in Fig. 2d–f. Obviously, the Fe/PdNi electrode with the atomic ratio of ~80/20 showed the highest oxidative peak current density to EOR (even higher than the Fe/Pd electrode). Elevating the Ni contents in the codeposits of PdNi did not show the advantage to the oxidative current densities of ethanol (Fig. 2d–f). One Fe/PdNi even showed a lower oxidative peak current density than the Pd wire electrode. The insets shown in Fig. 2d–f are SEM micrographs of the relevant electrode surfaces. Very interestingly, the Fe/PdNi electrode with the highest electrocatalytic activity ($Fe/Pd_{79}Ni_{21}$) exhibited the roughest surface. The surface was constituted of many islands formed from aggregated small particles and deep cracks were observed. Therefore, the morphologies of the PdNi surface might have a role as crucial as the compositions.

Sometimes, cyclic voltammograms were unable to show the more interior property of the electrocatalysts. Therefore, hydrodynamic amperometry was carried out in 1.0 M NaOH containing 1.0 M ethanol. Fig. 3a indicates that the introduction of Ni significantly suppressed the poisoning effect because all three Fe/PdNi

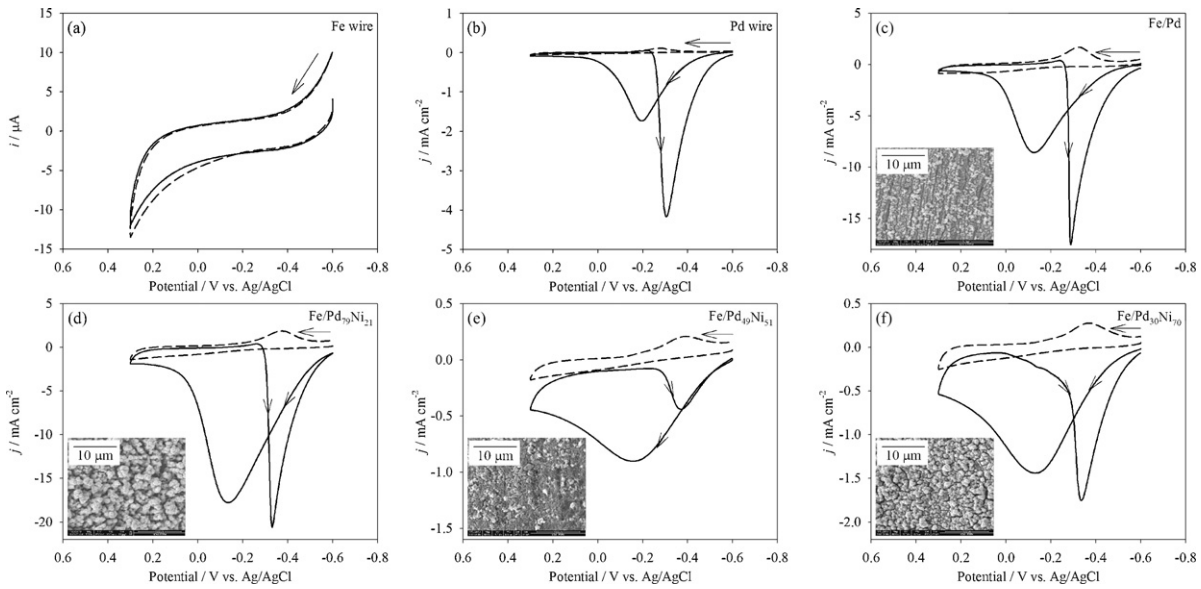

Fig. 2. Cyclic voltammograms recorded at various electrodes in 1.0 M NaOH with (—) and without (—) 1.0 M ethanol. The electrode used and the compositions of PdNi were indicated in each plot. The insets show the SEM micrographs of Pd- and three selected PdNi-coated electrodes. Scan rate: 50 mV s^{-1}.

electrodes showed higher oxidative current densities than the Fe/Pd electrode that demonstrated the second highest oxidative peak current density among the various electrodes (Fig. 2c); instead, the current transient recorded at the same Fe/Pd electrode decayed in the rapidest rate and approached to zero within 100s. Additionally, Fig. 3a indicates that elevating the atomic contents of Ni in the PdNi coatings indeed did not bring advantage to improve the electrocatalytic current in EOR. This behavior supports the published reports for ethanol oxidation on PdNi surfaces in alkaline solutions. Certain nickel oxides [25,26] such as NiO could enhance electrocatalytic activity and CO-resistance of Pd because the presence of oxides led to the formation of OH_{ads} (adsorbed OH species) at lower potential, which could transform the CO-like poisoning species adsorbed on catalyst to CO_2; the consequence was the release of active site for electrochemical reaction. However, too many nickel sites would dilute the Pd sites where oxidation of ethanol occurred.

Based on the cyclic voltammograms and the current transients shown in Figs. 2 and 3, the Fe/PdNi electrodes with the atomic ratio of ~80/20 were employed to study the dependence of the EOR currents on the concentration of ethanol ([Ethanol]). Two electrochemical methods, CV and HA, were performed for this study. Fig. 3b shows the cyclic voltammograms recorded at a $Fe/Pd_{75}Ni_{25}$ electrode in 1.0 M NaOH containing various concentrations of ethanol. Apparently, the oxidative peak currents of ethanol increased with increasing the ethanol concentrations. The inset of Fig. 3b shows the dependence of the oxidative peak currents (i_p) taken from the cyclic voltammograms on the ethanol concentration. Linearity was observed from 4.92 μM to 962 μM with a slope of 7.481 A M^{-1} and a regression coefficient of 0.995. The detection limit was 2.26 μM ($\sigma = 3$).

For hydrodynamic amperometric measurements (HA), a constant potential of −0.2 V (vs. Ag/AgCl) was applied at the $Fe/Pd_{78}Ni_{22}$ electrode immersed in the firmly stirred 1.0 M NaOH. The pure ethanol (99.9%) was successively injected and a limiting current (i_{ss}) was obtained after each injection (Fig. 3c). The value of the i_{ss} was employed to construct the calibration curve that is shown in the inset of Fig. 3c. The dependence of the i_{ss} on concentration of ethanol is linear from 4.92 μM to 988 μM with a slope of 0.8344 A M^{-1} and a regression coefficient of 0.9963. The detection limit was 0.83 μM ($\sigma = 3$).

3.3. Recovery test for ethanol

To assess the feasibility of the nonenzymatic electrochemical detection of ethanol using the Fe/PdNi electrodes, a recovery test was carried out in 1.0 M NaOH. A standard external calibration was performed to determine the ethanol concentrations added to the alkaline media. Two electrochemical methods, CV and HA, were employed to acquire the electrochemical signals. The experimental results were collected in Table 1. As can be seen, the recovery ratios from 89.30 to 105.43 were obtained. Low standard deviation

Table 1
Recovery test for ethanol and glucose using Fe/PdNi and SPC/Pd electrodes, respectively.

	Recovery test for ethanol				
	CV		HA		
Ethanol added (μM)	68.62		68.84		
Ethanol found after addition (μM)	72.35 ± 0.78		61.45 ± 0.28		
Recovery ratio (%)	105.43 ± 1.13		89.30 ± 0.41		
	Recovery test for glucose				
	SWV		CV		HA
Glucose added (mM)	5.682	0.092	5.682	0.085	1.690
Glucose found after addition (mM)	5.920 ± 0.050	0.091 ± 0.002	5.600 ± 0.010	0.087 ± 0.0003	1.600 ± 0.030
Recovery ratio (%)	104.2 ± 0.8	99.1 ± 2.2	98.6 ± 0.2	102.8 ± 0.4	94.9 ± 1.9

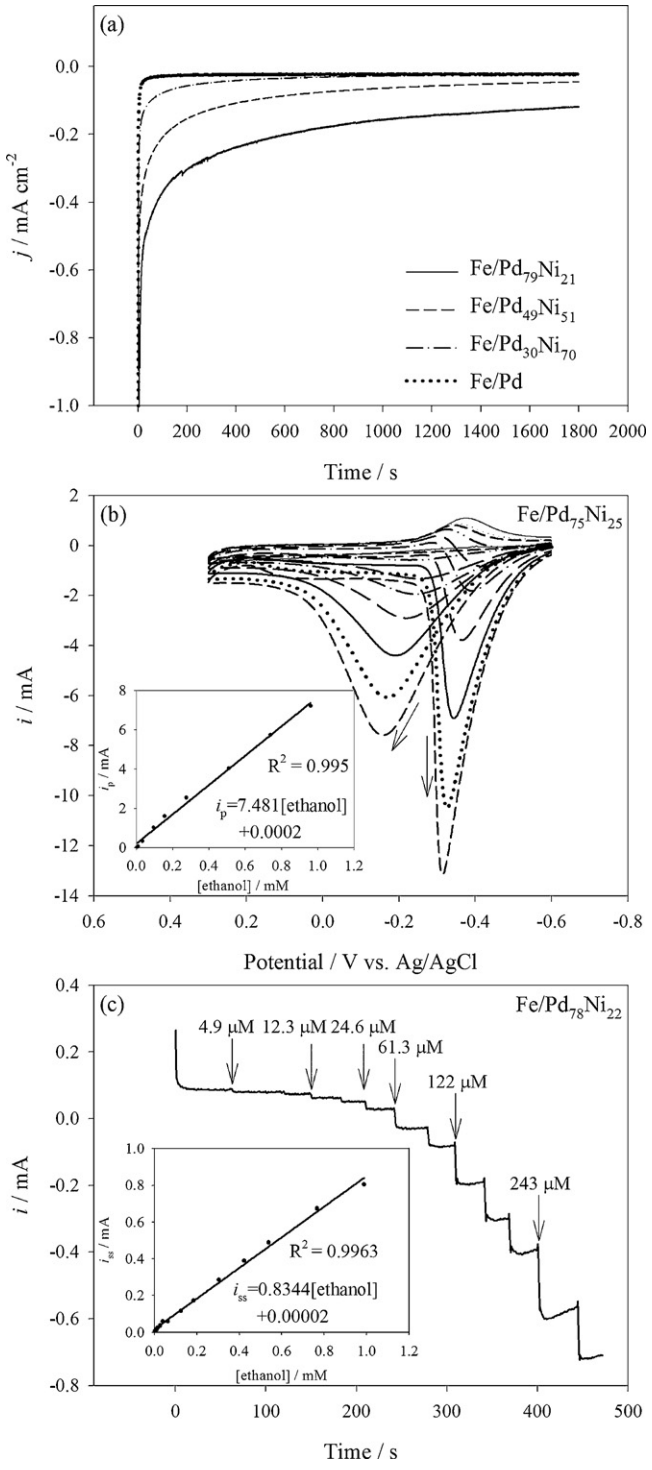

Fig. 3. (a) Hydrodynamic amperomograms recorded at four different electrodes in 1.0 M NaOH containing 1.0 M ethanol. Applied potential: −0.2 V. (b) Cyclic voltammograms recorded at the $Fe/Pd_{75}Ni_{25}$ electrode in 1.0 M NaOH containing various concentrations of ethanol. Scan rate: 50 mV s^{-1}. The inset shows the calibration curve of ethanol. (c) Hydrodynamic amperomogram recorded at the $Fe/Pd_{78}Ni_{22}$ electrode in 1.0 M NaOH where pure ethanol was successively injected and the relevant concentrations of ethanol were indicated. The inset shows the calibration curve of ethanol. Applied potential: −0.2 V.

indicated good precision; however, the accuracy obtained using HA was somewhat worse.

3.4. Nonenzymatic electrocatalytic oxidation of glucose at SPC/Pd electrodes

The electrodeposition of Pd (accumulating charge: 100 mC) was carried out in BMP-DCA containing 50 mM $PdCl_2$ by controlled-potential electrolysis on screen-printing carbon electrodes (SPC/Pd electrodes). The cyclic voltammograms recorded at the SPC/Pd in 0.1 M NaOH with and without 10 mM glucose are shown in Fig. 4a. Apparently, the SPC/Pd showed better electrocatalytic activity to glucose oxidation because lower overpotential was needed, compared with Ni electrodes that were usually employed for nonenzymatic glucose detection in alkaline solutions. The oxidation of glucose usually occurred at +0.4 to +0.6 V (vs. Ag/AgCl) on a Ni electrode. The oxidative peak current of glucose at the SPC/Pd increased with increasing the accumulating charge of Pd deposition; however, the signal transformed to a broad wave when the accumulating charge was higher than 200 mC. To extract signal from the background current became more difficult. Therefore, 100 mC of Pd was electrodeposited on a SPC electrode to prepare the SPC/Pd.

To further investigate the dependence of the glucose oxidation current on the concentration of glucose ([glucose]), the calibration curves were established by employing three electrochemical methods; CV, HA, and SWV. CV and SWV demonstrated better sensitivity and lower detection limit. The oxidative peak current (i_p) taken from the cyclic voltammograms and the square-wave voltammograms vs. the concentration of glucose demonstrated two linearities; one was observed in μM domain and the other one was observed in mM domain. HA showed a lower sensitivity and only one linearity was observed. The cyclic voltammograms recorded at an SPC/Pd in 0.1 M NaOH containing various concentrations of glucose and the relevant calibration curves are shown in Fig. S1. For HA measurements, a constant potential of −0.1 V (vs. Ag/AgCl) was applied at an SPC/Pd in a firmly stirred 0.1 M NaOH where the standard glucose solutions were successively injected and a limiting current (i_{ss}) was obtained after each injection (Fig. S2). A calibration curve was built using the i_{ss} (the inset of Fig. S2). The square-wave voltammograms recorded at an SPC/Pd electrode in 0.1 M NaOH containing different concentrations of glucose were shown in Fig. 4b and c. Fig. 4b showed the voltammograms corresponding to the lower concentration range of glucose. Oppositely, the voltammograms obtained at the higher concentration range of glucose is shown in Fig. 4c. The insets shown in Fig. 4b and c, respectively, indicate that good linearity was obtained at two concentration ranges. Therefore, the nonenzymatic electrochemical detection of glucose using the SPC/Pd electrodes should be feasible. To further verify whether the entire procedures are practicable, a recovery experiment was carried out. Three electrochemical methods SWV, CV, and HA were employed to determine the concentrations of glucose added to the 0.1 M NaOH. The experimental data were collected in Table 1. As can be seen, good recovery ratios from 94.9% to 104.2% were obtained with good precision (standard deviation < 2.2%).

3.5. Study of potentially interferential molecules in glucose detection, electrode stability, and determination of glucose in urine sample

Although this study focused on the determination of glucose in critical condition (that is in alkaline media), it is still interesting to know whether the SPC/Pd can be employed to detect glucose in physiological samples. For determination of glucose in real scenario, several molecules may be potentially interferential such as ascorbic acid (AA), uric acid (UA), and acetaminophen

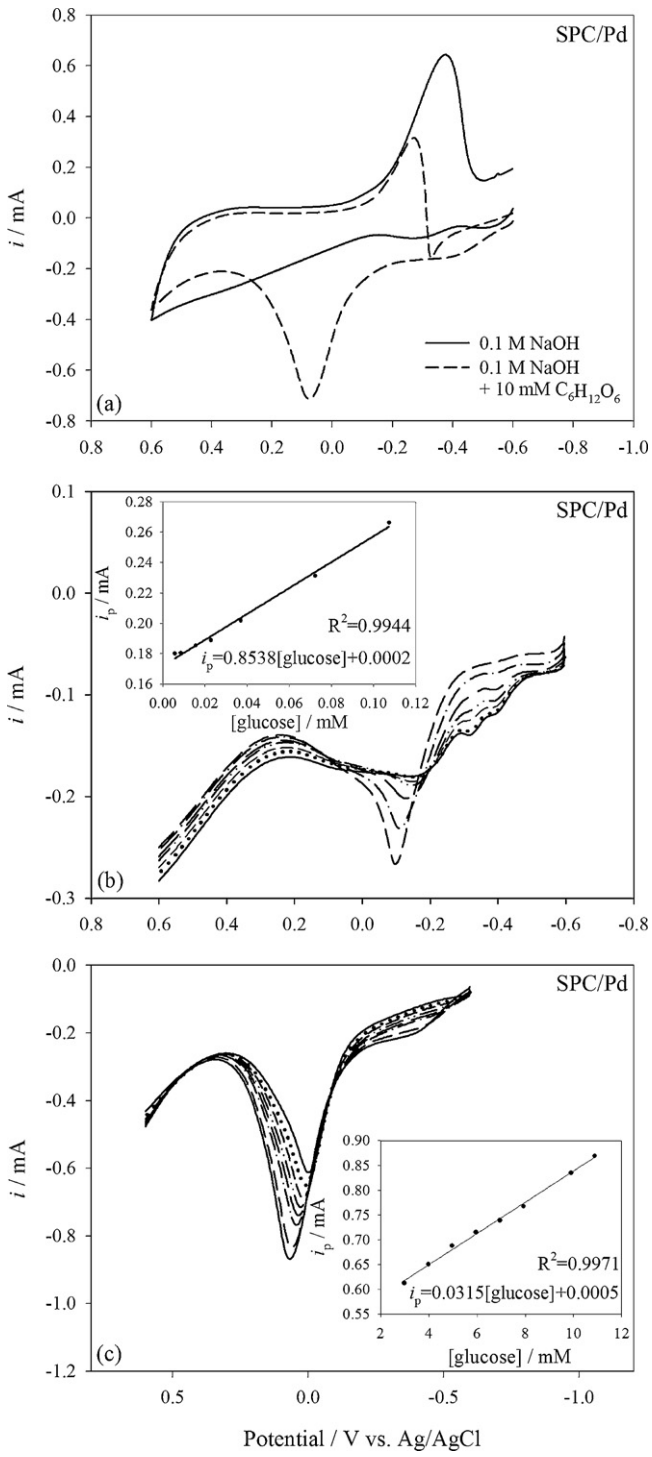

Fig. 4. (a) Cyclic voltammograms recorded at the SPC/Pd in 0.1 M NaOH with and without 10 mM glucose. Scan rate: 50 mV s^{-1}. (b) and (c) are square wave voltammograms recorded at the SPC/Pd in 0.1 M NaOH containing various concentrations of glucose. Parameters: amplitude = 0.025 V, increment potential = 0.004 V, and frequency = 15 Hz. The insets show the calibration curves of glucose.

(AP). Fig. 5a shows the cyclic voltammograms of glucose, AA, UA, and AP, respectively, recorded at the same SPC/Pd electrode in 0.1 M NaOH. Obviously, the SPC/Pd electrode showed the highest response to glucose and its current peak occurred at the most negative potential except for AA. Very unfortunately, the SPC/Pd prepared by electrodeposition from BMP-DCA seemed to simultaneously enhance the electrocatalytic activities towards glucose and AA because the two molecules were almost oxidized at the same

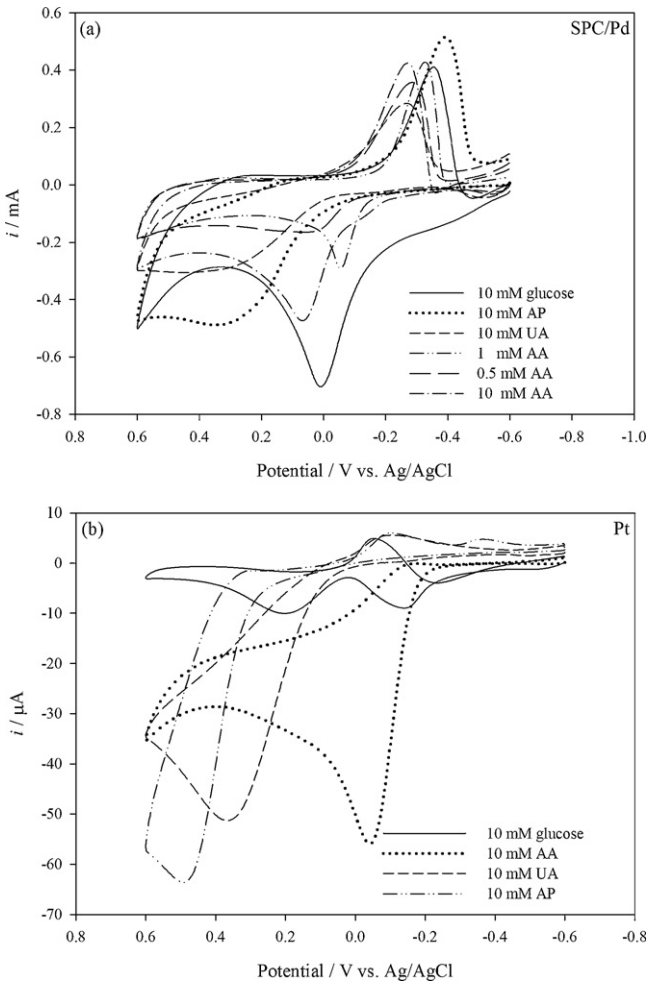

Fig. 5. Cyclic voltammograms recorded at (a) the SPC/Pd and at (b) the regular Pt disk electrode in 0.1 M NaOH containing various molecules indicated in each plots. Scan rate: 50 mV s^{-1}.

potential. However, at the same concentration, the SPC/Pd showed a higher response to glucose. Two lower concentrations of AA were detected and the oxidative currents apparently reduced. Based on the cyclic voltammograms shown in Fig. 5a and the difference of the physiological concentration between glucose and AA, the detection of glucose using the SPC/Pd should be resistant against the interferences.

Fig. 5b further emphasizes the predominance of the SPC/Pd over the regular Pt disk electrode. This figure shows the cyclic voltammograms of glucose, AA, UA, and AP, respectively, recorded at the same regular Pt disk electrode in 0.1 M NaOH. Two oxidative peaks related to glucose oxidation were observed at the Pt electrode; however, a single oxidative peak between the two peaks was observed at the SPC/Pd. Importantly and interestingly, the regular Pt disk electrode showed higher responses to all three interferential molecules and the lowest signal was observed for glucose oxidation. Reasonably, the Pt electrode should suffer by interference in detecting real samples.

An SPC/Pd was used to detect glucose in urine samples (from one volunteer of the group members) in which known concentrations of glucose (5 mM and 10 mM) were introduced and the solution pH was adjusted to 13.01 by the addition of NaOH. The recovery ratios obtained were 102.3 ± 9.62% and 82.3 ± 14.4%. Apparently, the electrode still suffered by certain interference in the physiological samples. There is still necessity to improve the performance of this electrode in the detection of glucose.

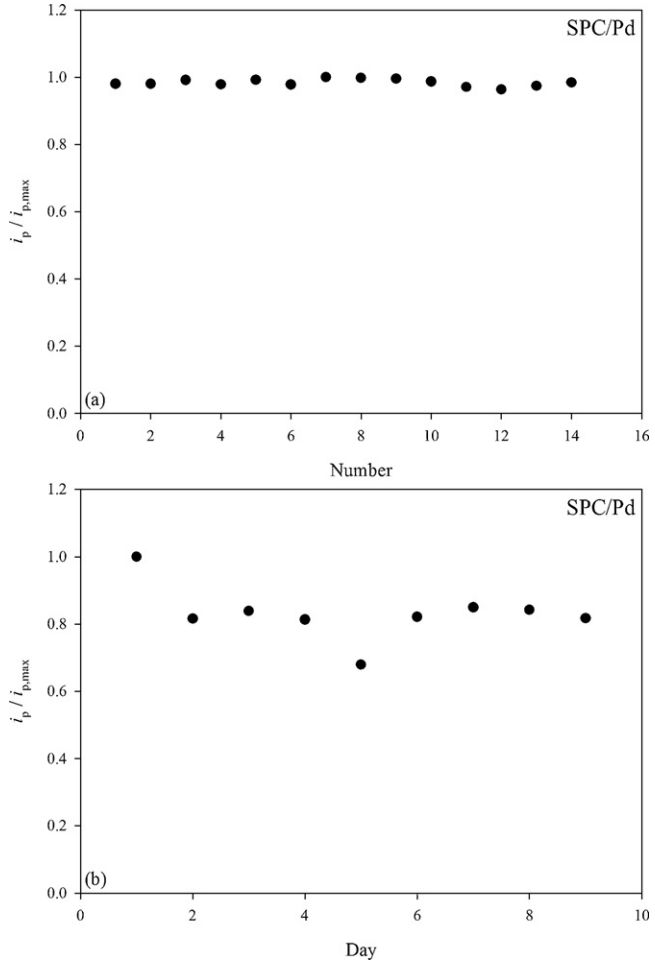

Fig. 6. Short-term stability and long-term stability of the SPC/Pd electrode in the detection of 5 mM glucose in 0.1 M NaOH solution.

Short-term stability (within 1 day) and relatively long-term stability (within 9 days) were examined at one SPC/Pd electrode in glucose determination (Fig. 6). This electrode showed an excellent short-term stability with the R.S.D. = 1.05% and an acceptable long-term stability with the R.S.D. = 9.22%. At the 9th day, the response current of glucose was still 82% of the 1st day's value. Actually, there was an outlier point in Fig. 6 that somehow might result from incautious work. The R.S.D. was 6.86% if this point is ignored. Additionally, except for the 1st day, the current response maintained within 81.3–84.9% of the 1st day's current.

4. Conclusion

Fe/PdNi and SPC/Pd were successfully prepared by the electrodeposition on Fe wire and SPC electrodes from the novel ionic liquid BMP-DCA where the widely separated reduction potentials of Pd(II) and Ni(II) in a regular aqueous solution overlapped in this IL. In addition, hydrogen evolution was prevented because this IL is aprotic. Hydrogen absorption on Pd surface can be avoided in this solvent when electrodeposition was employed to prepare Pd coatings. Fe/PdNi showed good sensitivity and poisoning resistance to ethanol determination. SPC/Pd showed good sensitivity to glucose determination; however, the resistance to interference has a space to be improved. This study provides a simple and fast method to prepare nonenzymatic electrodes for the determination of ethanol and glucose in critical conditions (in alkaline media) where enzyme electors usually lose their electrocatalytic activity. The two electrodes demonstrate a potency to be employed to nonenzymatic electrochemical determination of ethanol and glucose. However, for physiological determination of ethanol and glucose, these two electrodes must be improved because the two electrodes have to be used in alkaline conditions. It should be possible to prepare PdNi and Pd coatings constituted of nanoparticles by electrodeposition and IL can provide a good environment for codeposition of two metals with very different activity without hydrogen evolution and hydrogen adsorption.

Acknowledgments

The authors sincerely appreciate the financial support from the National Science Council of Taiwan (NSC98-2113-M-037-007-MY3) and the Center of Excellence for Environmental Medicine in Kaohsiung Medical University and the technical support from the instrumental center of National Cheng Kung University in Taiwan.

Appendix A. Supplementary data

Supplementary data associated with this article can be found, in the online version, at doi:10.1016/j.talanta.2010.09.032.

References

[1] A.M. Azevedo, D.M.F. Prazeres, M.S. Cabral, L.P. Fonseca, Biosens. Bioelectron. 21 (2005) 235.
[2] A. Heller, B. Feldman, Chem. Rev. 108 (2008) 2482.
[3] S. Park, H. Boo, T.D. Chung, Anal. Chim. Acta 556 (2006) 46.
[4] J.-F. Huang, Chem. Commun. (2009) 1270.
[5] H. Bai, M. Han, Y. Du, J. Bao, Z. Dai, Chem. Commun. 46 (2010) 1739.
[6] X.-M. Chen, Z.-J. Lin, D.-J. Chen, T.-T. Jia, Z.-M. Cai, X.-R. Wang, X. Chen, G.-N. Chen, M. Oyama, Biosens. Bioelectron. 25 (2010) 1803.
[7] L. Meng, J. Jin, G. Yang, T. Lu, H. Zhang, C. Cai, Anal. Chem. 81 (2009) 7271.
[8] F. Miao, B. Tao, L. Sun, T. Liu, J. You, L. Wang, P.K. Chu, Sens. Actuators B 141 (2009) 338.
[9] F. Xiao, F. Zhao, D. Mei, Z. Mo, B. Zeng, Biosens. Bioelectron. 24 (2009) 3481.
[10] F. Zhao, F. Xiao, B. Zeng, Electrochem. Commun. 12 (2010) 168.
[11] H. Zhu, X. Lu, M. Li, Y. Shao, Z. Zhu, Talanta 79 (2009) 1446.
[12] T.G. Satheesh Babu, T. Ramachandran, Electrochim. Acta 55 (2010) 1612.
[13] J.-W. Sue, C.-J. Huang, W.-C. Chen, J.-M. Zen, Electroanalysis 20 (2008) 1647.
[14] B. Tao, J. Zhang, S. Hui, L. Wan, Sens. Actuators B 142 (2009) 298.
[15] Z.X. Liang, T.S. Zhao, J.B. Xu, L.D. Zhu, Electrochim. Acta 54 (2009) 2203.
[16] E.E. Switzer, T.S. Olson, A.K. Datye, P. Atanassov, M.R. Hibbs, C.J. Cornelius, Electrochim. Acta 54 (2009) 989.
[17] X. Wang, W. Wang, Z. Qi, C. Zhao, H. Ji, Z. Zhang, Electrochem. Commun. 11 (2009) 1896.
[18] F. Endres, A.P. Abbott, D.R. MacFarlane, Electrodeposition from Ionic Liquids, Wiley-VCH, Weinheim, 2008.
[19] H. Ohno, Electrochemical Aspects of Ionic Liquids, John Wiley & Sons, New Jersey, 2005.
[20] J.L. Anderson, J. Ding, T. Welton, D.W. Armstrong, J. Am. Chem. Soc. 124 (2002) 14247.
[21] M.-J. Deng, P.-Y. Chen, T.-I. Leong, I.-W. Sun, J.-K. Chang, W.-T. Tsai, Electrochem. Commun. 10 (2008) 213.
[22] M.-J. Deng, I.-W. Sun, P.-Y. Chen, J.-K. Chang, W.-T. Tsai, Electrochim. Acta 53 (2008) 5812.
[23] D.R. MacFarlane, S.A. Forsyth, J. Golding, G.B. Deacon, Green Chem. 4 (2002) 444.
[24] M. Jayakumar, K.A. Venkatesan, T.G. Srinivasan, P.R. Vasudeva Rao, Electrochim. Acta 54 (2009) 6747.
[25] C. Xu, P.K. Shen, Y. Liu, J. Power Sources 164 (2007) 527.
[26] C. Xu, Z. Tian, P. Shen, S.P. Jiang, Electrochim. Acta 53 (2008) 2610.